J. Phys. Chem. A **2007,** *111,* 3069−3073 **3069**

Deuterium Isotope Effect on the Atomic Orbital Alignment Dependence in the Reaction of the Oriented Ar ($^3P_2$) with CH_3CN (CD_3CN)

Takashi Matsumura, Hiroshi Ohoyama,* Daisuke Watanabe, Keisuke Yasuda, and Toshio Kasai

Department of Chemistry, Graduate School of Science, Osaka University Toyonaka, Osaka 560-0043, Japan

Received: December 8, 2006; In Final Form: February 21, 2007

Atomic orbital alignment effect was observed for the CN ($B^2\Sigma^+$) formation in the reaction of oriented Ar ($^3P_2$) with CH_3CN (CD_3CN). The relative cross-sections for each magnetic M'_J substate in collision frame, $\sigma_H^{|M'_J|}$ for CH_3CN and $\sigma_D^{|M'_J|}$ for CD_3CN, were determined to be $\sigma_H^0{:}\sigma_H^{|1|}{:}\sigma_H^{|2|}{:}\sigma_D^0{:}\sigma_D^{|1|}{:}\sigma_D^{|2|} = 1.00{:}0.81{:}0.84{:}2.01{:}1.92{:}1.87$. A significant atomic orbital alignment effect was observed. In addition, a notable deuterium isotope effect was observed on both the cross-section and the atomic orbital alignment effect.

1. Introduction

The effect of atomic orbital alignment on reaction dynamics was first studied by Hertel et al. using an aligned Na (3^2P) prepared by optical pumping method.[1] Since then, the significant alignment dependences have been reported for the naked outer atomic orbitals in the singlet states prepared by optical pumping.[2−8] On the other hand, little is known about the steric aspect for the multiplet systems. Because the metastable rare gas atom has both the anisotropic electronic structure, $np^5(n+1)s^1$, due to an unpaired electron and the electric spins, it is important as a benchmark species to study the steric aspect for the multiplet systems.

Recently, we studied the steric effect in the Ar (^3P) + $N_2 \rightarrow N_2$ ($C,^3\Pi_u$) + Ar reaction by using an oriented Ar ($^3P_2$, $M_J = 2$) beam.[9] A significant atomic orbital alignment effect in the energy transfer process was observed. The alignment effect was qualitatively explained in terms of the anisotropy for the overlap efficiency between molecular orbital (MO) of N_2 and the unpaired inner atomic 3p orbital of Ar. In addition, it was revealed that the contribution of rank 4 moment is very small. The electron spin was found to have little effect on the dynamics as assumed by the Percival−Seaton hypothesis.[10] On the other hand, we observed a significant contribution of rank 4 moment in the dissociative energy transfer reaction of Ar ($^3P_2$) + $(X_2O)_2$ ($X = N$, H).[11] To study how the unpaired inner orbital of the triplet species interacts with the outer extended orbital in the course of electron exchange process, it is of great interest to compare the atomic orbital alignment effect with the effect on the molecular orientation in the same reaction system.

The reaction of metastable rare gas with small molecules has been widely studied as a benchmark model system to understand the fundamental reaction process such as electron and/or energy transfer.[12−16] Because this type of reaction is likely to be initiated by the electron exchange mechanism, the effects of molecular orientation in such processes have been observed in our laboratory.[17−20]

The reaction of Ar ($^3P_2$) + CH_3CN (CD_3CN) is one of the widely studied reaction systems so far.[17−18,21−24] The cross-section of CN(B) formation in the CH_3CN +Ar* reaction has been determined to be a few A^2.[22,23] While, the total quenching cross-section of Ar* by CH_3CN has been determined to be $160A^2$ in the nearly thermal energy region.[24] The comparison of the cross-section for CN(B) formation with $160A^2$ gives an estimation of the low branching fraction for CN(B) formation. These results are quite parallel to the small quantum yield for the production of CN(B) observed in the vacuum ultraviolet (VUV) photodissociation[25] and support that the CN(B) formation is competitive with other fast exit channels. The main channel of the title reaction is estimated to be the H-elimination.

For these reactions, we studied the molecular orientation dependence for the CN ($B^2\Sigma^+$) formation by using the oriented CH_3CN (CD_3CN) beam.[17−18] From the large stereoanisotropy observed in the CN ($B^2\Sigma^+$) formation for the reaction with oriented CH_3CN, we suggested the important contribution of the $7a_1$ orbital, which is localized at the CN group. In addition, we observed the deuterium isotope effect on the molecular orientation dependence and the cross-section. We attributed the deuterium isotope effects on the cross-section to the dissociation dynamics itself from the excited states because the energy transfer probability depends only on the electronic term and has no isotope effect. For the increment of the reaction probability by the deuteration of CH_3CN, we argued that the deuteration of the molecule reduces the CD vibrational frequency and make D-elimination compete less effectively with CN(B) formation after the energy transfer has occurred. In addition, the increment of the reaction probability by the deuteration of CH_3CN showed a nearly isotropic behavior on molecular orientation. From these results, we suggested that the additional process is attributed to the reaction relevant to 2e molecular orbital that has the spatial distribution spreading over the sideways direction. In other words, it was proposed that the CN ($B^2\Sigma^+$) formation has at least two reaction processes relevant to the different two molecular orbitals, $7a_1$ and 2e.[18]

Since the effect of molecular orientation for the reaction of Ar ($^3P_2$) + CH_3CN (CD_3CN) was already studied in our previous study,[18] it is of great interest to compare the atomic orbital alignment effect with the effect on the molecular orientation in this reaction system. In the present study, we study the atomic orbital alignment effect and its deuterium isotope effect in the reaction of Ar ($^3P_2$) + CH_3CN. A significant atomic orbital alignment effect is observed. In addition, a notable deuterium

---

* To whom correspondence should be addressed. E-mail: ohyama@chem.sci.osaka-u.ac.jp.

10.1021/jp068440l CCC: $37.00

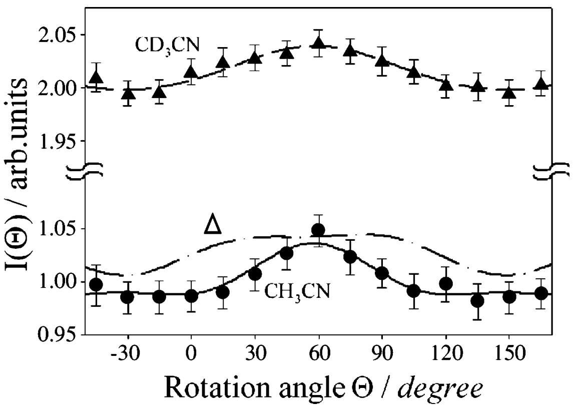

Figure 1. The chemiluminescence intensity of CN ($B^2\Sigma^+$), $I_{H(D)}(\Theta)$, as a function of the orientation field direction Θ for the reaction of CH_3CN (circle), CD_3CN (triangle), and the increment Δ of the cross-section by the deuteration of CH_3CN (dashed-and-dotted line). The lines are the Θ-dependences reproduced by using eq 3 for CH_3CN (solid line), CD_3CN (dashed line). The origin of the rotation angle Θ is defined as the direction of Ar ($^3P_2$) beam axis. The direction of the relative velocity vector Θ_{VR} is 58.0° (58.4°) for the CH_3CN (CD_3CN) reaction.

isotope effect is observed on both the cross-section and the atomic orbital alignment effect. The deuterium isotope effect on the atomic orbital alignment effect is discussed by comparing with that on the molecular orientation effect.

2. Experimental Section

Details of the experimental apparatus and the procedure are the same as other studies described elsewhere[9,11,19,26] and only an outline is given here. A metastable Ar ($^3P_{0,2}$) beam was generated by a pulsed glow discharge with a pulse width of 100 μs. An inhomogeneous permanent magnetic hexapole was used to generate the M_J state-selected Ar ($^3P_2$) beam that is composed of almost pure Ar ($^3P_2$, M_J (**B**) = 2) state (more than 93%) in the magnetic field **B**.[26] A CH_3CN (CD_3CN) beam was injected from a pulsed valve with a stagnation pressure of 7 Torr. The CH_3CN (CD_3CN) was used after the purification by the vacuum degassing procedure with the freeze−thaw cycles. The M_J state-selected Ar ($^3P_2$, M_J (**B**) = 2) beam collided with the CH_3CN (CD_3CN) beam in the homogeneous magnetic orientation field **B**. The direction of the magnetic orientation field **B** was rotated around the beam crossing point over the angle region $-45 \leq \Theta \leq 165°$ by an interval of 15°. The origin of Θ is the direction of the Ar ($^3P_2$) beam axis. The chemiluminescence from the product CN ($B^2\Sigma^+$) at the beam crossing point was selectively collected by a concave mirror and detected by a cooled and magnetic-shielded photomultiplier (Hamamatsu R943−02) mounted at 30 cm apart from the beam crossing point through a suitable band-pass filter (HOYA U340 & L-39). As reported in our previous study,[9] the state-selected Ar($^3P_2$) with the specific velocity of around 700 ms^{-1} consists of almost pure $M_J = 2$ component. To collect only the signal from this specific velocity region, the signal from the photomultiplier was counted by a multichannel scaler (Stanford SR430) for the sake of time-of-flight analysis. The chemiluminescence was measured as a function of the direction of the magnetic orientation field in the laboratory frame (rotation angle Θ).

3. Results

3.1. M_J' dependent cross-section, $\sigma|M_J'|$. Figure 1 shows the chemiluminescence intensity of the product CN ($B^2\Sigma^+$) in the title reactions, $I_{H(D)}(\Theta)$, as a function of the orientation field direction Θ. Here, the subscript symbols of H and D label the system as the CH_3CN and CD_3CN reactions, respectively. It is easily found that the CH_3CN and CD_3CN reactions give the different Θ-dependence. A notable deuterium isotope effect is observed on both the cross-section and the atomic orbital alignment effect.

To extract the quantitative information on the isotope effect, we adapt the evolution procedure based on an irreducible representation of the density matrix. The detail of the analytical procedures and the derivation of all the algebra are reported elsewhere.[21−22] In general, the Θ-dependence of the chemiluminescence intensityI(Θ) can be expressed by

$$I(\Theta) = \frac{D\bar{I}}{(2J+1)} \sum_{kq} g_k(J) S_{kq}(\mathrm{B,J}) T_{kq}(\mathrm{B,J}) \qquad (1)$$

where S_{kq}(B,J) and T_{kq}(B,J) are the real multipole moments of the density matrix of the prepared oriented Ar ($^3P_2$, M_J (**B**) = 2) atom and of the collision density matrix respectively, D is an experimental detection efficiency, $\bar{I}$ is the polarization averaged cross-section, and $g_k(J)$ are numerical factors.

In the present study, the general eq 1 can be simplified as the following equation:

$$\begin{aligned} I_{H(D)}(\Theta) = {} & \frac{1}{280}(39\sigma^0_{H(D)} + 88\sigma^{|1|}_{H(D)} + 153\sigma^{|2|}_{H(D)}) \\ & + \frac{1}{16}(-3\sigma^0_{H(D)} - 4\sigma^{|1|}_{H(D)} + 7\sigma^{|2|}_{H(D)})\langle\cos(2\theta)\rangle \\ & + \frac{1}{64}(3\sigma^0_{H(D)} - 4\sigma^{|1|}_{H(D)} + \sigma^{|2|}_{H(D)})\langle\cos(4\theta)\rangle \end{aligned} \qquad (2)$$

where θ is the angle between the relative velocity v_R and the direction of the orientation magnetic field **B**. It is defined as $\theta \equiv \Theta_{VR} - \Theta$ using the direction of the relative velocity v_R in the laboratory coordinate, Θ_{VR}. Because this angle has a distribution by the misalignment caused by the velocity distribution of CH_3CN (CD_3CN) beam, we must use the cos 2nθ factors averaged over the Maxwell−Boltzmann velocity distribution of CH_3CN (CD_3CN) beam at room temperature, $\langle\cos(2n(\Theta_{VR} - \Theta))\rangle$.

This equation is equivalent to the following multipole moment form

$$I_{H(D)}(\Theta) = a_{0,H(D)} + a_{2,H(D)}\langle\cos 2(\Theta_{VR} - \Theta)\rangle + a_{4,H(D)}\langle\cos 4(\Theta_{VR} - \Theta)\rangle \quad (3)$$

The parameters, $a_{n,H(D)}$, are determined by the fitting of $I_{H(D)}(\Theta)$ using eq 3. The relative cross-section, $\alpha_{H(D)} \equiv \sigma^{|1|}_{H(D)}/\sigma^0_{H(D)}$ and $\beta_{H(D)} \equiv \sigma^{|2|}_{H(D)}/\sigma^0_{H(D)}$, can be derived from the experimental coefficient ratio of $a_{2,H(D)}/a_{0,H(D)}$ and $a_{4,H(D)}/a_{0,H(D)}$. By using the relative cross-sections, $\alpha_{H(D)}$ and $\beta_{H(D)}$, $I_{H(D)}(\Theta)$ can be rewritten as

$$\begin{aligned} I_{H(D)}(\Theta) = \sigma^0_{H(D)}\Big[& \frac{1}{280}(39 + 88\beta_{H(D)} + 153\alpha_{H(D)})\Big] \\ & + \frac{1}{16}(-3 - 4\beta_{H(D)} + 7\alpha_{H(D)})\langle\cos 2(\Theta_{VR} - \Theta)\rangle \\ & + \frac{1}{64}(3 - 4\beta_{H(D)} + \alpha_{H(D)})\langle\cos 4(\Theta_{VR} - \Theta)\rangle \end{aligned}$$

Because the relative cross-section, σ^0_H/σ^0_D, can be determined by comparing the intensity between $I_H(\Theta)$ and $I_D(\Theta)$, all the

TABLE 1: The Ratio of $a_{2,H(D)}/a_{0,H(D)}$ and $a_{4,H(D)}/a_{0,H(D)}$, and the Relative Cross-Sections $\sigma_{H(D)}^{|M_J'|}/\sigma_H^0$ for the Ar ($^3P_2$) + CH_3CN (CD_3CN) Reactions

	CH_3CN	CD_3CN	Δ
$a_{2,H(D)}/a_{0,H(D)}$	$-(2.4 \pm 0.3) \times 10^{-2}$	$-(2.1 \pm 0.2) \times 10^{-2}$	
$a_{4,H(D)}/a_{0,H(D)}$	$(1.1 \pm 0.4) \times 10^{-2}$	$(0.17 \pm 0.29) \times 10^{-2}$	
$\sigma_{H(D)}^0/\sigma_H^0$	1.00	2.01 ± 0.08	1.01 ± 0.08
$\sigma_{H(D)}^{\|1\|}/\sigma_H^0$	0.81 ± 0.04	1.92 ± 0.09	1.11 ± 0.13
$\sigma_{H(D)}^{\|2\|}/\sigma_H^0$	0.84 ± 0.03	1.87 ± 0.07	1.03 ± 0.10
$\sigma_{H(D)}(CN)/\sigma_H(CH_3)^a$	2.9	4.7	1.8
$\sigma_{H(D)}(CH_3)/\sigma_H(CH_3)^a$	1.0	3.0	2.0

[a] Cited from ref 18.

cross-sections $\sigma_{H(D)}^{|M'_J|}$ can be determined as the relative cross-sections to σ_H^0 as

$$\sigma_H^0:\sigma_H^{|1|}:\sigma_H^{|2|}:\sigma_D^0:\sigma_D^{|1|}:\sigma_D^{|2|} = 1.00:0.81:0.84:2.00:1.95:1.87.$$

They are summarized in Table 1. A notable isotope effect is observed on both the cross-section and the alignment effect. The reaction of CH_3CN is slightly favorable for the collision with the configuration of $M_J' = 0$. It is found that the reaction of CD_3CN is more isotropic than the reaction of CH_3CN. To compare the previous result for the effect on the molecular orientation,[18] for convenience, we separate the cross-section $\sigma_{M_J'}^D$ into two parts

$$\sigma_D^{M_J'} = \sigma_H^{M_J'} + \Delta^{M_J'}$$

where $\Delta^{M_J'}$ are the increments of the cross-section by the deuteration of CH_3CN. They are also shown in Figure 2. It is found that $\Delta^{M_J'}$ is slightly favorable for the collision with the configuration of $|M_J'| = 1$. As the references, the deuterium isotope effects on the molecular orientation dependence cited in ref. 18 are shown in Table 1. It is revealed that there is some configurational correlation between the atomic orbital alignment and the molecular orientation.

4. Discussion

4.1. Overview of the Reaction Mechanism of Ar ($^3P_2$) + CH_3CN (CD_3CN). A number of studies have been carried out for the reaction of Ar ($^3P_2$) + CH_3CN (CD_3CN). This reaction is known as a dissociative energy transfer reaction expressed by[15,19]

$$\text{Energy transfer: } Ar\ (^3P_2) + CH_3CN \rightarrow CH_3CN^* + Ar\ (^1S_0)$$

$$\text{Dissociation: } CH_3CN^* \rightarrow CN\ (B^2\Sigma^+) + CH_3.$$

The electron configuration of the ground CH_3CN (CD_3CN) is expressed as $(core)^6(4a_1)^2(5a_1)^2(6a_1)^2(1e)^4(7a_1)^2(2e)^4$[4,24,27] On the basis of the electron impact energy loss spectrometry and the VUV absorption spectra,[25,28,29] it is expected that $7a_1$ and/or 2e orbital can interact with the 3p orbital of Ar ($^3P_2$).

There are two possible pathways for the energy transfer processes:

Path 1: $7a_1$ orbital → Rydberg orbitals, npσ and/or ndσ

Path 2: 2e orbital → Rydberg orbitals, nsσ, npσ, npπ and ndσ

It has been suggested that the energy transfer proceeds via the following electron-exchange process:

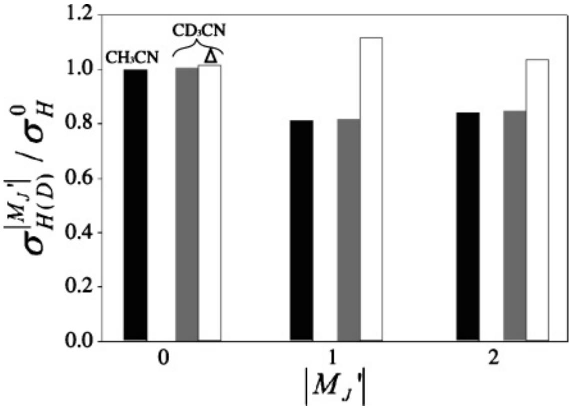

Figure 2. The M_J'-resolved relative cross-section $\sigma_H^{|M_J'|}$ for CH_3CN (filled bar), and $\sigma_D^{|M_J'|}$ for CD_3CN ($\sigma_H^{|M_J'|}$ (shadow bar) + $\Delta^{|M_J'|}$ (open bar)). Open bar expresses the increment Δ by the deuteration.

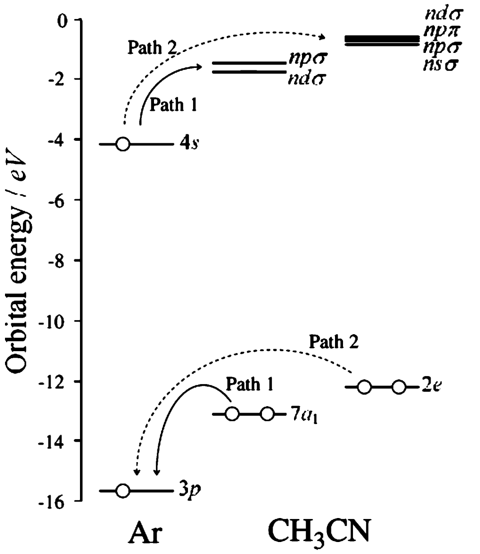

Figure 3. Schematic diagram of two candidates for the electron exchange processes, path 1 and path 2. The orbital energies on the energy transfer via the electron exchange for Ar and CH_3CN.

Step 1. The electron in the relevant MO of the molecule transfers to the half-filled 3p orbital of Ar ($^3P_2$).

Step 2. The 4s electron of Ar ($^3P_2$) transfers to an empty Rydberg orbital of the molecule.

The electron exchange processes for the above pathways are illustrated in Figure 3. If the interaction between 3p and 4s is ignorable, the transition matrix element is given by[30,31]

$$V_{if} = \langle \varphi_i | H_{el} | \varphi_f \rangle \approx \langle 3p(1)Ryd(2) | 1/r_{12} | MO(1)4s(2) \rangle \quad (4)$$

where H_{el} is the electronic Hamiltonian, and φ_i and φ_f are electronic wavefunctions for the initial and the final states, respectively, 4s and MO are the 4s orbital of Ar ($^3P_2$) and the molecular orbital of CH_3CN in the initial states, respectively, and 3p and Ryd are the 3p orbital of Ar and the orbital of CH_3CN in the final state, respectively. On the basis of the Mulliken approximation for the two electron integral,[32] the steric effect for the transition matrix is approximated by the probability of orbital overlap.[31] In particular, we must consider the orbital overlap between the 3p orbital of Ar ($^3P_2$) and the MO of CH_3CN (CD_3CN) in the step 1 because the step 2 is expected to be more isotropic than the step 1.

4.2. Characteristics of Potential Energy Surface. To make clear the origin of deuterium isotope effect and the steric effect,

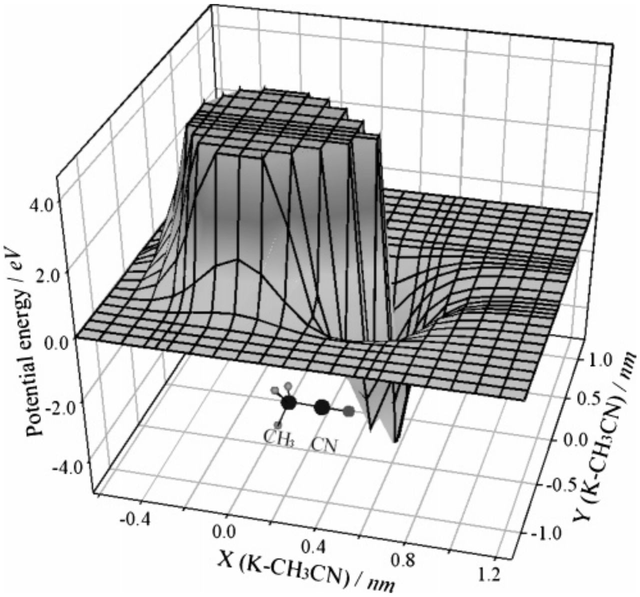

Figure 4. A model potential K + CH_3CN for Ar ($^3P_2$) + CH_3CN by using a ground state K atom instead of a Ar ($^3P_2$). The calculations were performed by the GAUSSIAN 98 ab initio program package using the Hartree−Fock method with 6-31G basis set.

we have to know about the potential energy surface (PES) for Ar ($^3P_2$) + CH_3CN. Unfortunately, it is difficult to obtain reliable interaction energy by the ab initio treatments of Ar ($^3P_2$) associated with highly excited electronic states. Because Ar ($^3P_2$) has the same outer valence electronic configuration as K with the 4s electron that mainly contributes to the interactions, the similarity between Ar ($^3P_2$) and K is expected. For the qualitative understanding of the interaction potential, we roughly calculate the model potential K + CH_3CN for Ar ($^3P_2$) + CH_3CN by using a ground state K atom instead of an Ar ($^3P_2$). The calculations are performed by the Hartree−Fock method with 6-31G basis set. The potential energy V is obtained by the following manner

$$V = E_{(\mathrm{K+CH_3CN})} - (E_\mathrm{K} + E_\mathrm{CH_3CN})$$

$E_{(\mathrm{K+CH_3CN})}$, E_K, and $E_\mathrm{CH_3CN}$ are the total energy of the super molecule (K−CH_3CN), the isolated K atom, and the isolated CH_3CN, respectively.

The calculated model PES is shown in Figure 4. It is found that the interaction potential is attractive around the CN group, while it is repulsive around the CH_3 group. The collision from the CH_3 group is expected to be less reactive due to the steric hindrance by the repulsive wall.

4.3. Deuterium Isotope Effect on the Atomic Orbital Alignment Dependence. The deuterium isotope effect on the atomic orbital alignment dependence directly indicates that the reaction has at least two reaction pathways for the formation of CN ($B^2\Sigma^+$). This result is consistent with the previous report for the deuterium isotope effect on the molecular orientation dependence for the CN ($B^2\Sigma^+$) formation. In the previous study, we suggested that the two reaction pathways are the path 1 and the path 2. If the path 2 is the origin of the increment Δ, the path 2 must be less dependent on the molecular orientation and slightly favorable for the collision with $|M_J'| = 1$ configuration.

To discuss the steric effect on the electron transfer from the MO of CH_3CN to the 3p orbital of Ar, we calculate the distribution of the "exterior electron" for the MO of CH_3CN by using the GAUSSIAN 98 ab initio program package with 6-311++G(3df, 2pd) basis set.

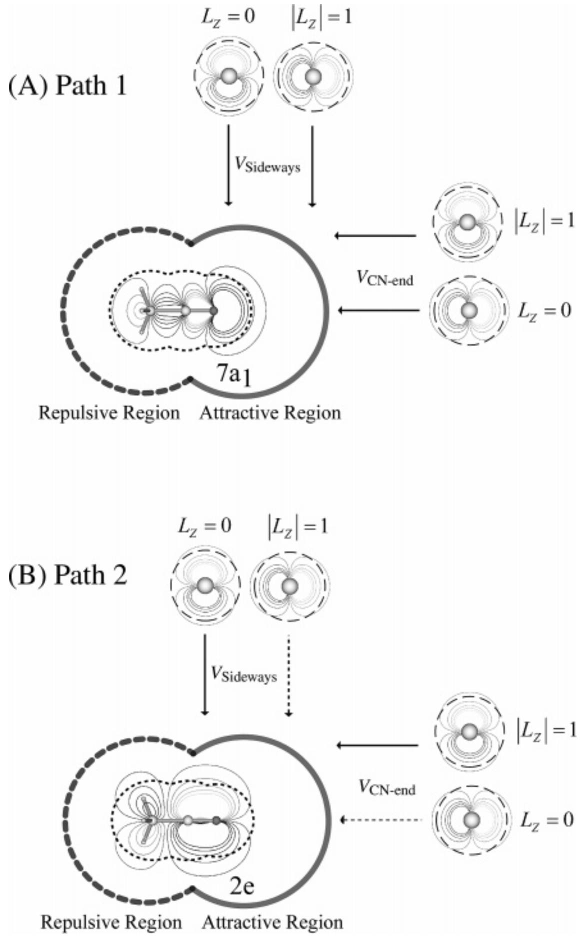

Figure 5. The distribution of the exterior electron for the $7a_1$ and 2e molecular orbital of CH_3CN that are relevant to the two electron exchange processes, path 1 (A) and path 2 (B), and for the 3p orbital of Ar. The distributions were calculated by using the GAUSSIAN 98 ab initio program package with 6-311++G (3df, 2pd) basis set. Inner broken lines express van der Waals radius as an approximate position of the repulsive wall. The arrows indicate the representative collision directions for favorable collision (solid arrow), unfavorable collision (broken arrows).

The calculated electron density distribution for the $7a_1$ and 2e molecular orbitals is shown in Figure 5A,B, respectively.

On the basis of the simple consideration about characteristics of the PES and the symmetry of the orbital, we can deduce the efficiency for the interaction between MO and 3p orbital. From the repulsive characteristics of the PES around the CH_3 group, it is expected that the collision from the CH_3-end is less reactive. In other words, only the collision from the CN-end and the sideways direction are reactive.

Steric Effect in the Path 1. For the path 1, we must consider the steric effect on the orbital overlap between the 3p orbital of Ar and the $7a_1$ molecular orbital of CH_3CN (CD_3CN) as shown in Figure 5A. For the collisions from both the CN-end and sideways directions, the configuration of $L_Z = 0$ is favorable at small impact parameter, while the configuration of $|L_Z| = 1$ is favorable at large impact parameter. These results are in good agreement with both the large molecular orientation dependence and the slight atomic orbital alignment dependence on the reaction of CH_3CN.

Steric Effect in the Path 2. If the path 2 is the origin of the increment Δ, the path 2 must be less dependent on the molecular orientation and slightly favorable for the collision with $|M_J'| = 1$ configuration.

For the path 2, we must consider the steric effect on the orbital overlap between the 3p atomic orbital of Ar and the 2e molecular orbital of CH_3CN (CD_3CN) as shown in Figure 5B. The CN-end collision with the configuration of $L_Z = 0$ should be unfavorable because the 2e orbital has a nodal plane along the molecular axis. On the other hand, the CN-end collision with the configuration of $|L_Z| = 1$ at large impact parameter is likely to have an efficient overlap. For the sideways collision, the configuration of $L_Z = 0$ is favorable, while the configuration of $|L_Z| = 1$ is expected to be unfavorable. Therefore, it is unlikely that the path 2 shows the lack of the dependence on molecular orientation.

If the path 2 is the origin of the increment Δ, this process must have no dependence on the molecular orientation. This restriction imposes that only the sideway collision must dominantly contribute to the path 2. Even in such a case, however, the prediction by the orbital overlap conflicts with the almost isotropic experimental atomic orbital alignment dependence for the increment Δ because the sideway collision should be favorable for the configuration of $L_Z = 0$. As a result, it is unlikely that the path 2 is the one responsible for Δ.

It seems to be difficult to explain the deuterium isotope effect on both the atomic orbital alignment and the molecular orientation dependence by the static anisotropy for the orbital overlap efficiency between MO and 3p orbital. In other words, the more complicated considerations including the effect of spin and/or the dynamical effect are necessary. Unfortunately, it is hard to make a rigorous theoretical treatment of the dynamics including the effect of spin. In such cases, the rank 4 moment (a_4) should be an important indicator to know the spin interaction between the electron in the unpaired inner atomic 3p orbital and that in the outer extended 4s orbital, because no contribution of rank 4 moment (a_4) directly signifies that the dynamics is dominantly determined by the orbital angular momentum L and its components L_Z without spin interaction. As listed in Table 1, we observe the substantial contribution of rank 4 moment (a_4) for the CH_3CN. This result indicates that the step 1 should have some correlation with the step 2. In other words, the excited Rydberg states themselves after energy transfer should depend on the M_J' component of Ar ($^3P_2$) and/or the molecular orientation. To explain the observed deuterium isotope effect on both the atomic orbital alignment and the molecular orientation dependence, we must assume the correlation between the excited Rydberg states and the molecular orientation and/or the atomic orbital alignment. That is, the different excited Rydberg states should be produced depending on the molecular orientation. In such assumption, the observed deuterium isotope effects suggest that the excited Rydberg states produced from the sideways collision is less efficient for the D-elimination as compared with those produced from the CN-end collision.

5. Conclusions

Atomic orbital alignment effect was observed for the CN ($B^2\Sigma^+$) formation in the reaction of oriented Ar ($^3P_2$) with CH_3CN (CD_3CN). A notable deuterium isotope effect was observed on both the cross-section and the atomic orbital alignment effect. Some configurational correlations between the atomic orbital alignment and the molecular orientation were revealed. In addition, it was suggested that the spin interaction between the unpaired inner orbital and the outer extended orbital in the triplet species and/or the dynamical effect give a significant effect on the stereoselectivity for the electron exchange processes.

References and Notes

(1) Hertel, I. V.; Hofmann, H.; Rost, K. A. *Phys. Rev. Lett.* **1977**, *38*, 343.

(2) Rettner, C. T.; Zare, R. N. *J. Chem. Phys.* **1981**, *75*, 3636.

(3) Rettner, C. T.; Zare, R. N. *J. Chem. Phys.* **1982**, *77*, 2416.

(4) Smith, C. J.; Spain, E. M.; Daiberth, M. J.; Leone, S. R.; Driessen, J. P. J. *J. Chem. Soc., Faraday Trans.* **1993**, *89*, 1401.

(5) Campbell, E. E. B.; Hulser, H.; Witte, R.; Hertel, I. V. *Z. Phys. D. At., Mol. Clusters* **1990**, *16*, 21.

(6) Robinson, R. L.; Kovalenko, L. J.; Smith, C. J.; Leone, S. R. *J. Chem. Phys.* **1990**, *92*, 5260.

(7) Driessen, J. P. J.; Smith, C. J.; Leone, S. R. *J. Phys. Chem.* **1991**, *95*, 8163.

(8) Campbell, E. E. B.; Schmidt, H.; Hertel, I. V. *Adv. Chem. Phys.* **1998**, *72*, 37.

(9) Watanabe, D.; Ohoyama, H.; Matsumura, T.; Kasai, T. *J. Chem. Phys.* **2006**, *125*, 084316.

(10) Percival, I. C.; Seaton, M. J. *Proc. Cambridge Philos. Soc.* **1957**, *53*, 654.

(11) Watanabe, D.; Ohoyama, H.; Matsumura, T.; Kasai, T. *J. Chem. Phys.*, in press.

(12) Gundel, L. A.; Setser, D. W.; Clyne, M. A. A.; Coxon, J. A.; Nip, W. *J. Chem. Phys.* **1976**, *64*, 4390.

(13) Velazco, J. E.; Kolts, J. H.; Setser, D. W. *J. Chem. Phys.* **1978**, *69*, 4357.

(14) Balamuta, J.; Golde, M. F. *J. Chem. Phys.* **1982**, *76*, 2430.

(15) DeVries, M. S.; Tyndall, G. W.; Cobb, C. L.; Martin, R. M. *J. Chem. Phys.* **1986**, *84*, 3753.

(16) Johnson, K.; Pease, R.; Simons, J. P. *Mol. Phys.* **1984**, *52*, 955.

(17) Kasai, T.; Che, D. C.; Ohashi, K.; Kuwata, K. *Chem. Phys. Lett.* **1989**, *163*, 246.

(18) Che, D. C.; Kasai, T.; Ohoyama, H.; Ohashi, K.; Fukawa, T.; Kuwata, K. *J. Phys. Chem.* **1991**, *95*, 8159.

(19) Ohoyama, H.; Kasai, T.; Ohashi, K.; Kuwata, K. *Chem. Phys.* **1992**, *65*, 155.

(20) Ohoyama, H.; Makita, H.; Kasai, T.; Kuwata, K. *J. Phys. Chem.* **1995**, *99*, 5798.

(21) Kanda, K.; Igari, N.; Kikuchi, Y.; Kishida, N.; Igarashi, J.; Katsumata, S. *J. Phys. Chem.* **1995**, *99*, 5269.

(22) Tabayashi, K.; Shobatake, K. *J. Chem. Phys.* **1987**, *87*, 2404.

(23) Sadeghi, S.; Setser, D. W. *Chem. Phys. Lett.* **1981**, *82*, 44.

(24) Bourene, M.; LeCalve, J. *J. Chem. Phys.* **1973**, *58*, 1452.

(25) Kanda, K.; Nagata, T.; Ibuki, T. *Chem. Phys.* **1999**, *243*, 89.

(26) Watanabe, D.; Ohoyama, H.; Matsumura, T.; Kasai, T. *Eur. Phys. J. D* **2006**, *38*, 219.

(27) Minchinton, A.; Brion, C. E.; Cook, J. P. D.; Weigold, E. *Chem. Phys.* **1983**, *76*, 81.

(28) Ashfold, M. N. R.; Simons, J. P. *J. Chem. Soc., Faraday Trans 2* **1978**, *74*, 1263.

(29) Fridh, C. *J. Chem. Soc., Faraday Trans. 2* **1978**, *74*, 2193.

(30) Takahashi, H.; Ohoyama, H.; Kasai, T.; Nakano, M.; Yamaguchi, K. *J. Phys. Chem.* **1995**, *99*, 13600.

(31) Ohno, K. *Bull. Chem. Soc. Jpn.* **2004**, *77*, 887.

(32) Mulliken, R. S. *J Chim. Phys.* **1949**, *46*, 497.